Self-catalysis in the gas-phase: enolization of the acetone radical cation

Moschoula A. Trikoupis [a], Peter C. Burgers [b], Paul J.A. Ruttink [c], Johan K. Terlouw [a,*]

[a] *Department of Chemistry, McMaster University, Hamilton, Ont., Canada, L8S 4M1*
[b] *Hercules European Research Center, Hercules B.V., P.O. Box 252, 3770 AG, Barneveld, The Netherlands*
[c] *Theoretical Chemistry Group, Department of Chemistry, University of Utrecht, Padualaan 14, 3584 CH, Utrecht, The Netherlands*

In memory of Professor Pierre Longevialle, truly a Maître de Recherche.

Abstract

Because of a prohibitively large barrier, the solitary acetone radical cation, $CH_3C(=O)CH_3^{\bullet+}$ ($1^{\bullet+}$) does not rearrange, neither spontaneously nor by activation, to its more stable enol isomer, $CH_2=C(OH)CH_3^{\bullet+}$ ($1a^{\bullet+}$). However, this isomerization occurs smoothly by an ion–molecule interaction with neutral acetone itself. The dimer radical cation, $[1^{\bullet+}\cdots 1]$, generated under conditions of chemical ionization dissociates to m/z 58 and collision-induced dissociation (CID) experiments show that these ions have the enol structure $1a^{\bullet+}$. Labeling experiments indicate that the reaction can be viewed as a simple 1,3-hydrogen shift within the acetone radical cation of the complex. Ab initio calculations at the CBS-Q/DZP level of theory indicate that this isomerization is best described as a proton transport catalysis rather than as a spectator model. Our calculations show that the incipient radical formed during the proton abstraction is not $CH_3C(=O)CH_2^{\bullet}$, but rather the less stable configuration $CH_3C(-O^{\bullet})=CH_2$ stabilized by $CH_3C(OH)CH_3^{+}$. This behaviour can be rationalized by arguments based on ion-dipole interactions. The incipient radical $CH_3C(-O^{\bullet})=CH_2$ is transformed to its more stable configuration $CH_3C(=O)CH_2^{\bullet}$ via surface crossing. However, this process does not occur via the usual "minimum to minimum crossing" but rather by the novel process of "transition state to minimum crossing". The abstracted proton is then donated back to the oxygen atom of $CH_3C(=O)CH_2^{\bullet}$ to yield the hydrogen-bridged radical cation $[1a^{\bullet+}\cdots 1]$. The observed tautomerization of the acetone radical cation by acetone itself can be viewed as "self-catalysis". (Int J Mass Spectrom 217 (2002) 97–108) © 2002 Elsevier Science B.V. All rights reserved.

Keywords: Proton transfer catalysis; Tandem mass spectrometry; Enolization; Dimer radical cation; Ab initio calculations; Surface crossing

1. Introduction

The mass spectrometer has long been recognized as the instrument of choice to study isomerization and dissociation reactions of solitary ions. In the words of Professor Longevialle: "... le spectromètre de masse... joue le double rôle de réacteur (ionisation des molécules, fragmentation, etc.) et d'analyseur des produits de la réaction" [1]. Over the past 40 years, numerous studies have appeared dealing with the unimolecular chemistry of isolated ions, in particular radical cations, and as a result of these investigations we think that today we have a reasonable understanding of the properties of such species. If

---

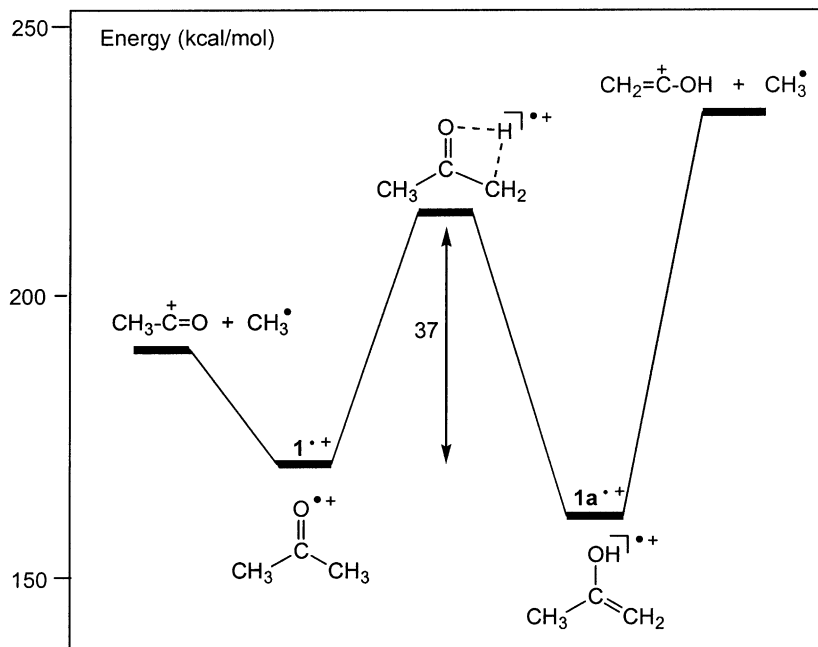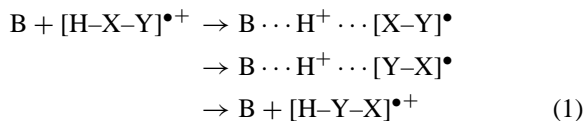* Corresponding author. E-mail: terlouwj@mcmaster.ca

Fig. 1. Energy diagram for the isomerization and dissociation of acetone keto and enol radical cations.

there is one thing that chemists have learned from these studies it is that one-electron oxidation can drastically change the chemistry of the system. For example, simple neutral enols are thermodynamically less stable than their keto isomers, but the opposite is true for the corresponding radical cations. A case in point is acetone. Experiments show that the gaseous acetone radical cation is 14 kcal/mol [2] less stable than its enol isomer, paralleling observations from theory [3]. However, a large barrier of 37 kcal/mol for the 1,3-hydrogen shift [4] prevents enolization, and thus once formed, the acetone radical cation retains its structure. The energy diagram for the keto–enol acetone radical cation tautomerization is given in Fig. 1 and note that even energized acetone ions will not isomerize; rather they will dissociate by loss of $CH_3^\bullet$.

Recently, experimental [5] and theoretical [6] studies have reported a mechanism by which a gaseous conventional radical cation can rearrange to a more stable isomer via a two-step proton transfer through interaction with an appropriate base B according to Eq. (1).

$$
\begin{aligned}
B + [H–X–Y]^{\bullet+} &\rightarrow B \cdots H^+ \cdots [X–Y]^\bullet \\
&\rightarrow B \cdots H^+ \cdots [Y–X]^\bullet \\
&\rightarrow B + [H–Y–X]^{\bullet+} \quad\quad (1)
\end{aligned}
$$

This process has been termed "proton transport catalysis" [5a]. The process not only occurs under certain conditions of bimolecular reactions (see below), but it also plays a key role in the dissociation of a variety of oxygen-containing radical cations [7]. The first studies of proton transport catalysis of radical cations [5b–d] focused on isomers separated by a 1,2-H shift, such as $CH_3OH^{\bullet+}$ which by interaction with a suitable base can rearrange into its more stable yield isomer, $CH_2OH_2^{\bullet+}$, $X = CH_2$ and $Y = OH$ in Eq. (1). More recent experiments and ab initio calculations [5e,5i] show that 1,3-H shifts can also be catalyzed by interaction with a suitable base molecule although the associated mechanism is not always that

of a true proton transport catalysis [5i]. For example, the acetone radical cation rearranges smoothly to its enol via interaction with benzonitrile (BN) [5e], $X = CH_2$ and $Y = C(=O)CH_3$ in Eq. (1) via proton transfer catalysis.

Gauld and Radom [6b] have evaluated conditions for efficient proton transport catalysis. First, and as indicated in Eq. (1), the base should be able to abstract a proton from the radical cation. Secondly, the incipient protonated base should be able to donate back this same proton, but at a different site. That is to say, efficient catalysis will take place only when the proton affinity (PA) of the base lies between the PA of [X–Y] at X and at Y. Using this criterion, we concluded that BN should be a suitable candidate for a base and indeed, subsequent experiments showed that BN can catalyze the enolization of the acetone radical cation [5e].

However, during an evaluation of criteria for successful catalysis of 1,3-H shifts in a variety of radical cations, we noted an interesting, and possibly general, phenomenon. Taking acetone as an example, we observed that the PA of the incipient radical $[CH_2C(O)CH_3]^\bullet$ at oxygen is virtually identical to the PA of acetone itself, viz 196 kcal/mol. This simple observation indicates that acetone itself would be a suitable candidate to catalyze the 1,3-H shift in its partner radical cation. By contrast, 1,2-H shifts may not be catalyzed by the neutral molecule itself. For example, the PA of CH_3OH (180 kcal/mol [8]) is much larger than the PA of $CH_2OH^\bullet$ at O (166 kcal/mol [8]) and so in this case proton abstraction of $CH_3OH^{\bullet+}$ by CH_3OH will be unidirectional leading to $CH_3OH_2^+$ only. There is another mechanism by which 1,2-H and 1,3-H shifts may be induced to occur by the encounter with a neutral base molecule. If the barrier for the unassisted reaction is not too large, then an ion-dipole interaction of the radical cation with the "base" may produce sufficient stabilization in itself to lower the unassisted barrier to below the separated starting components, thus promoting rearrangement. This is called the "spectator" mechanism and we do not know of any experimental method to differentiate between this mechanism and a "true" proton transport catalysis.

(For a description of the spectator model vs. proton transport catalysis, see [5f].) However, a decision between the mechanisms can be made on the basis of ab initio calculations, vide infra.

In this report, we present our results on the catalysis of the enolization of the acetone radical cation by acetone itself. Our experiments show that acetone can indeed catalyze this isomerization and our ab initio calculations show that the associated mechanism is a "true" proton transport catalysis as opposed to a spectator process. We consider such a reaction whereby an acetone molecule catalyses enolization of its partner radical cation an example of "self-catalysis" as defined by Clennan et al. [9]. Thus, the starting species, neutral acetone is oxidized to its radical cation which then undergoes a further reaction catalyzed by the starting material. By contrast, in an autocatalytic process it is a reaction product which acts as catalyst.

2. Experimental and theoretical methods

All experiments were performed with the McMaster University VG Analytical (Manchester, UK) ZAB-R instrument of $B_1E_1E_2$ geometry (B, magnet; E, electric sector). Metastable ion (MI) mass spectra were recorded in the second field free region (2ffr); collision-induced dissociation (CID) mass spectra were recorded in the 2ffr and 3ffr using oxygen as collision gas (transmittance 70%). The CID mass spectra of the 2ffr metastable or CID peaks were obtained in the 3ffr using oxygen as collision gas. The accelerating voltage used was 8 kV, except for the reference acetone and enol spectra which were obtained using 4 kV. This was done to ensure that the reference ions and product ions resulting from MI or CID have the same translational energies. All spectra were recorded using a small PC-based data system developed by Mommers Technologies Inc. (Ottawa).

All compounds were of research grade and were used without further purification. The dimer radical cations were generated as follows: under conditions of chemical ionization, the acetone radical cation, readily and preferentially undergoes proton transfer to acetone

Table 1
Electronic energies (Hartree), scaled zero-point vibrational energies (ZPVEs, kcal/mol) and relative energies, E_{rel} (kcal/mol), of the species involved in the acetone assisted enolization of the acetone radical cation

Species	RHF/DZP	ZPVE	CBS-Q/DZP	E_{rel}
$CH_3C(=O)CH_3$, **1**	−192.00868	56.2	−192.82080	
$CH_3C(=O)CH_3^{•+}$, **1$^{•+}$**	−191.69909	55.5	−192.46038	0
$CH_2=C(OH)CH_3^{•+}$, **1a$^{•+}$**	−191.71279	56.4	−192.47648	−10.1
$CH_3C(=O)CH_2^{•}$, **[1 − H]$^{•}$**	−191.37823	47.2	−192.16828	
$CH_3C(-O^{•})=CH_2$, **[1 − H]$_\alpha^{•}$**	−191.35477	47.7	−192.15709	
$CH_3C(OH)CH_3^{+}$, **[1 + H]$^{+}$**	−192.33943	64.9	−193.12670	
TS(**1$^{•+}$** → **1a$^{•+}$**)	−191.60130	52.4	−192.40404	35.3
1 + **1$^{•+}$**	−383.70777	117.7	−385.28118	0
1 + **1a$^{•+}$**	−383.72147	112.6	−385.29728	−10.1
Complex **2$^{•+}$**	−383.73128	112.6	−385.30689	−16.1
TS(**2$^{•+}$** → **3a$^{•+}$**)	−383.70023	110.0	−385.29036	−5.8
Complex **3a$^{•+}$**	−383.71013	113.7	−385.29347	−7.7
TS(**3a$^{•+}$** → **3$^{•+}$**)	−383.70693	113.4	−385.29742	−10.2
PGCP[a]	−383.70706	–	−385.46737	−16.3
Complex **3$^{•+}$**	−383.76335	112.9	−385.34341	−39.1
TS(**3$^{•+}$** → **4$^{•+}$**)	−383.76164	110.2	−385.35012	−42.6
Complex **4$^{•+}$**	−383.76529	113.2	−385.34469	−39.9
[1 − H]$_\alpha^{•}$ + **[1 + H]$^{+}$**	−385.69420	112.6	−385.28379	−1.6
[1 + H]$^{•}$ + **[1 + H]$^{+}$**	−383.71766	112.1	−385.29498	−8.7
TS spectator mechanism	−383.64105	109.6	−385.25647	15.5

[a] No ZPVE included, the CBS-Q/DZP total energy for **1**+**1$^{•+}$** = −385.44137 Hartree.

(self-protonation) to produce $CH_3C^{+}(OH)CH_3$, a reaction which is exothermic by 15 kcal/mol [8]. However, we observed that this side reaction can be largely suppressed by using CS_2 as a bath gas in the ion source, at a pressure of 1×10^{-4} Torr. The CS_2 is added to the source through a capillary and the pressure is held constant with the use of a Negretti valve. The pressure of acetone was held at 1×10^{-6} Torr. We also tried methyl iodide as a bath gas but because of its lower ionization energy (IE = 9.54 eV) compared to that of acetone (9.71 eV), the acetone ions are neutralized. By contrast, CS_2 has a higher IE (10.07 eV) [8].

Standard ab initio molecular orbital calculations were performed with the Gaussian 98 [10] and GAMESS-UK [11] systems of programs. Stationary points on the potential energy surface (PES) were calculated using RHF/DZP. Frequency calculations gave the correct number of eigenvalues for all minima and transition states reported. Unless otherwise stated, the spin contamination was acceptable, within 10% of

0.75. Final energies were obtained by the CBS-Q [12] procedure to obtain the results presented in Table 1.

3. Results and discussion

3.1. The acetone molecule assisted isomerization of the acetone radical cation **1$^{•+}$**, experimental observations

The major dissociation observed in the MI mass spectrum of the acetone dimer radical cation [**1$^{•+}$** ⋯ **1**], involves the formation of the monomer "acetone" cation. A smaller peak (ca. 30%) is found at m/z 59 corresponding to $CH_3C^{+}(OH)CH_3$, **[1 + H]$^{+}$**, the result of a unidirectional proton transfer, i.e., a proton transfer immediately followed by dissociation. Dissociations, characteristic of the acetone monomer radical cation, viz. the losses of $CH_3^{•}$ and CH_4 [13] are absent for the dimer radical cation. The energy requirement for formation of m/z 59 from

the dimer radical cation is 105 kcal/mol (from ΔH_f $[1 + H]^+ = 117$ kcal/mol [8] and ΔH_f $[^\bullet CH_2C(=O)CH_3] = -12$ kcal/mol [5e]. If m/z 58 corresponds to ionized acetone, then the calculated threshold energy is 120 kcal/mol (from ΔH_f $[1^{\bullet+}] = 172$ kcal/mol [8] and ΔH_f $[1] = -52$ kcal/mol [8]. However, if m/z 58 has the enol structure $1a^{\bullet+}$, the energy requirement becomes 106 kcal/mol (from ΔH_f $[1a^{\bullet+}] = 158$ kcal/mol [8]. However, it cannot be concluded from these data that the m/z 58 product ion has the enol structure, because formation of m/z 59, even though this reaction is a simple proton transfer, may be associated with a forward barrier [5i]. Therefore, it was decided to probe the structure of the m/z 58 ions by CID experiments. In Fig. 2a and b are given the reference CID mass spectra of the keto and enol forms respectively and these spectra are characteristically different in the m/z 24–31 region. In Fig. 2c is given the CID mass spectrum of the m/z 58 ions generated from the metastable dimer radical cation and this spectrum leaves no doubt that the metastably dissociating dimer radical cations produce the enol ions $1a^{\bullet+}$. The question now arises: do the non-decomposing ions also isomerize into an [enol acetone$^{\bullet+}\cdots$acetone] complex ? This is an important question, because an answer, either way, would provide an indication as to the height of the barrier.

In our previous study [5e] on the BN catalyzed enolization of the acetone ion $1^{\bullet+}$, we had concluded that for the non-decomposing ions, the initially formed $[1^{\bullet+}\cdots BN]$ complex completely rearranges, via proton transport catalysis, to the complex cation $[1a^{\bullet+}\cdots BN]$, the very stable hydrogen-bridged radical cation $[CH_2=C(CH_3)-O\cdots H\cdots N\equiv C-C_6H_5]^{\bullet+}$. If the acetone dimer radical cation behaves in the same way, then the initially formed $[1^{\bullet+}\cdots 1]$ complex will have completely rearranged in the microsecond time-frame to the adduct $[1a^{\bullet+}\cdots 1]$, the hydrogen-bridged radical cation $[CH_2=C(CH_3)-O\cdots H\cdots O=C(CH_3)_2]^{\bullet+}$. Upon collisional activation, the complex will then yield m/z 58 ions having the enol of acetone structure as this is the energetically most favourable dissociation of the $[1a^{\bullet+}\cdots 1]$ complex. Experiments are in complete agreement
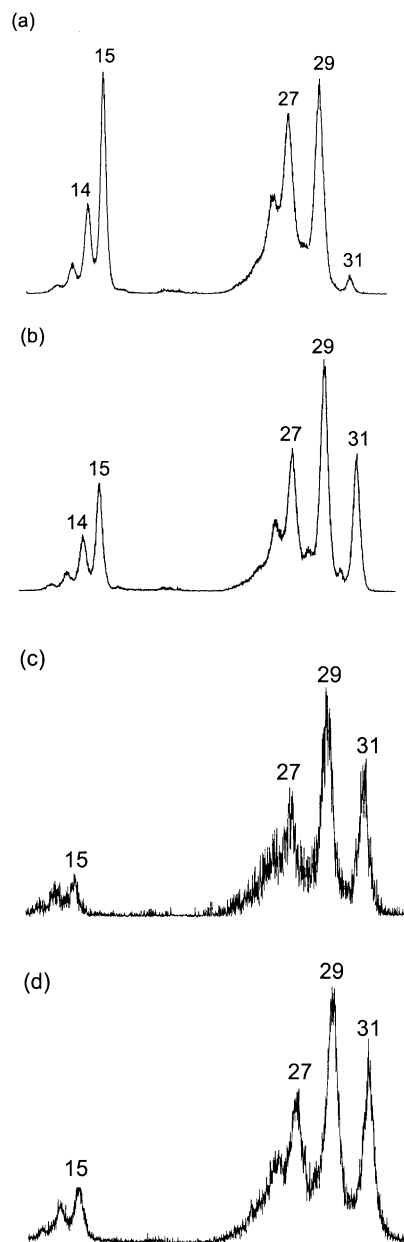

Fig. 2. 8 keV CID mass spectra of: (a) acetone; (b) enol of acetone; (c) the metastably generated m/z 58 ions from the $[CH_3C(=O)CH_3]_2^{\bullet+}$ complex; (d) the collisionally formed m/z 58 ions from the $[CH_3C(=O)CH_3]_2^{\bullet+}$ complex.

with this hypothesis: the CID mass spectrum of the collisionaly generated m/z 58 ions recorded in an MS/MS/MS experiment, see Fig. 2d, shows that pure enol ions are produced. Thus, stable complex cations $[1^{\bullet+} \cdots 1]$ also completely rearrange to the adduct ion $[1a^{\bullet+} \cdots 1]$ on the microsecond time-scale. This experiment shows that the barrier for isomerization within the complex lies lower than the energy for the separated components, $1^{\bullet+} + 1$.

The mixed labeled dimer ion $[CD_3C(=O)CD_3 \cdots CH_3C(=O)CH_3]^{\bullet+}$, where the charge may be on either moiety, was also investigated and its partial MI spectrum is given in Fig. 3. It can be seen that the m/z 58 signal is split into m/z 58 and 64 peaks, precisely as expected on the basis of proton transport catalysis (or the spectator model). CID experiments on the metastable mixed labeled dimer ion showed that m/z 58 and 64 correspond to pure enol ions as was the case for the unlabeled dimer ion. It can also be seen that m/z 60, $CH_3C(OD)CH_3^+$ which results from the competing process of complete D^+ abstraction is significantly weaker than m/z 65 $CD_3C(OH)CD_3^+$ which results from H^+ abstraction. This shows that complete proton transfer from one partner to another is associated with a significant isotope effect; thus this simple proton transfer may well be associated with a significant barrier. It is of interest to note that the unidirectional proton transfer suffers from an appreciable isotope effect (as evidenced by the ratio m/z 60:65), but that no such isotope effect appears to operate in the enolization process. However, if it is assumed that the second
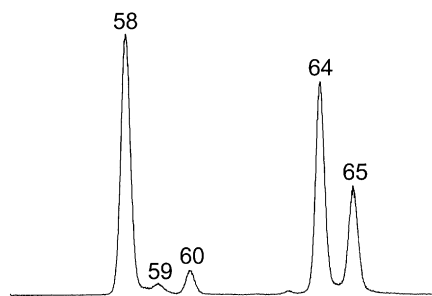
proton transfer, i.e., the donation back of the abstracted proton, suffers from a similar isotope effect, then both effects cancel out and an intensity ratio of 1 is expected for m/z 58 and 64. Apart from the expected peaks at m/z 58, 60, 64 and 65, there are also minor signals at m/z 59 and 63. These minor products we propose arise by isomerization via a process which involves a sequential proton and a hydrogen (or deuterium atom) transfer within the $[1^{\bullet+} \cdots 1]$ complex as is the case for the isomerization of ionized acetamide using BN as base [5i]. These minor processes were not further investigated.

3.2. Theoretical calculations

An important energetic constraint to guide us in our ab initio calculations is provided by the MS/MS/MS experiment described above and that is that the barrier for the catalyzed isomerization should lie below the energy of the separated starting components, $1^{\bullet+} + 1$. This finding will become important when we need to decide between proton transport catalysis and a spectator model. For ionized acetone, proton transport catalysis involves the following sequence. The acetone radical cation $1^{\bullet+}$ reacts with neutral acetone, 1, to give the initial complex $[1^{\bullet+} \cdots 1]$, ion $2^{\bullet+}$ in Scheme 1. This complex then undergoes proton transfer to generate the complex $[1-H]^{\bullet} \cdots [1+H]^+$, $3^{\bullet+}$, which then donates back the proton to generate the final complex $[1a^{\bullet+} \cdots 1]$, $4^{\bullet+}$, which then dissociates to the enol of acetone radical cation, $1a^{\bullet+}$, and 1. The competing process of unidirectional proton transfer leads to $CH_3C^+(OH)CH_3$ and $CH_3C(=O)CH_2^{\bullet}$, $[1+H]^+$ and $[1-H]^{\bullet}$.

The characterization of the PES was started by performing RHF/DZP calculations to locate the stationary points for the proton transport catalysis model: i.e., the reaction sequence $2^{\bullet+} \rightarrow TS(2 \rightarrow 3)^{\bullet+} \rightarrow 3^{\bullet+} \rightarrow TS(3 \rightarrow 4)^{\bullet+} \rightarrow 4^{\bullet+}$. According to these calculations the ions $3^{\bullet+}$ and $4^{\bullet+}$ are quite stable species. The transition $3^{\bullet+} \rightarrow 4^{\bullet+}$ has a very low activation energy as may be expected for an $O \cdots H^+ \cdots O$ proton transfer. Ion 2 has a stabilization energy of 16 kcal/mol. The structures encountered on the surface are shown in Scheme 1. It is of interest to note that from the
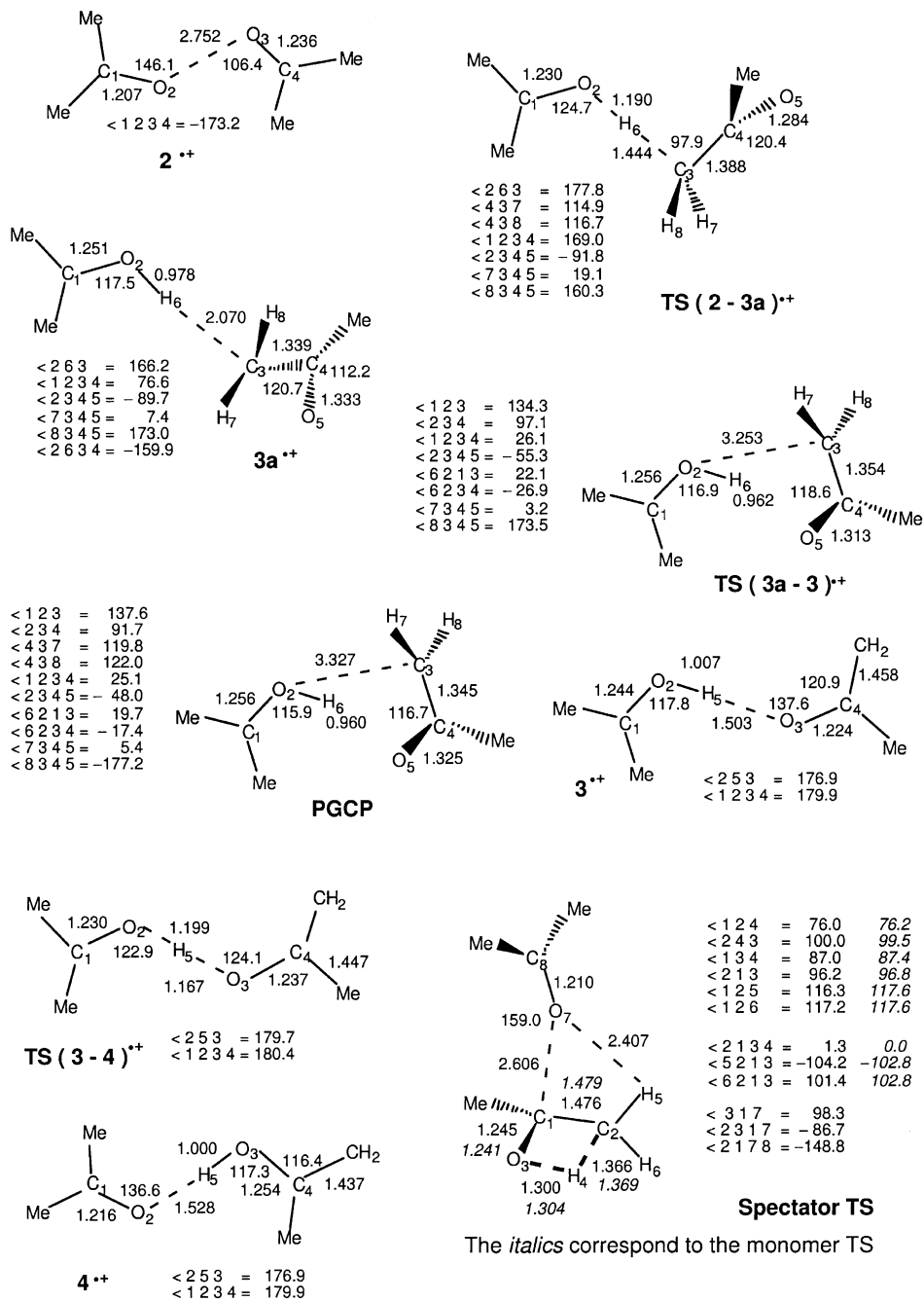

Fig. 3. 8 keV MI mass spectrum of the m/z 122 $[CH_3C(=O)CH_3/CD_3C(=O)CD_3]^{\bullet+}$ complex ion.
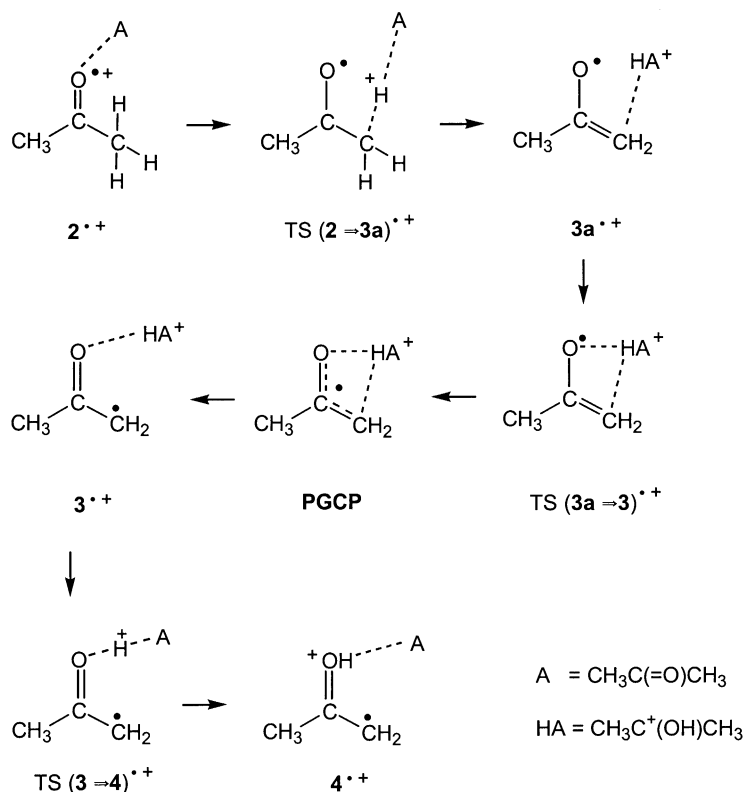
Scheme 1.

structure of TS($2 \rightarrow 3a$)$^{•+}$ in Scheme 2, it may be inferred that the H shift is indeed a proton shift and not an H atom shift. If it were an H atom shift then the dipole vector of the right-hand neutral species would point to the wrong direction. The calculated energies are shown in Table 1 and the energy diagrams derived therefrom are given in Fig. 4.

Since the first step should also correspond to a proton transfer, the transition was expected to feature a structure like [CH$_3$C(=O)CH$_2$$^{•}$···H$^+$···O=C(CH$_3$)$_2$]. However, a TS of this form could not be found. This may be rationalized by the fact that a structure of the above form has no electrostatic stabilization after passing the transition state; this is because the vector of the dipole moment of the radical moiety points in the wrong direction. However, another possibility for the transition $2^{•+} \rightarrow 3^{•+}$ originates from the idea that the deprotonated acetone radical [$1 - H$]$^{•}$ may have two electronic configurations, i.e., the normal, low energy form CH$_3$C(=O)CH$_2$$^{•}$ and the alternative, higher energy form CH$_3$C(O$^{•}$)=CH$_2$, [$1 - H$]$_\alpha$$^{•}$, which features a small C=CH$_2$ distance and a large C–O distance. This leads to a TS of the form [CH$_3$C(O$^{•}$)=CH$_2$···H$^+$···O=C(CH$_3$)$_2$], TS($2^{•+} \rightarrow 3a^{•+}$) in Schemes 1 and 2. This structure has some stabilization from the interaction of the positive charge on the protonated acetone with the C=C double bond of the alternative form of the radical, [$1 - H$]$_\alpha$$^{•}$. A geometry optimization starting from this TS leads to ion $3a^{•+}$ with almost the same geometry (apart from the H$^+$–O distance) and an energy just below the TS($2^{•+} \rightarrow 3a^{•+}$) energy. The next step would be to find a TS for the transition CH$_3$C(–O$^{•}$)=CH$_2$ $\rightarrow$ CH$_3$C(=O)CH$_2$$^{•}$ in the radical moiety of the complex. However, this TS could not be found. TS searches for the above transition for the
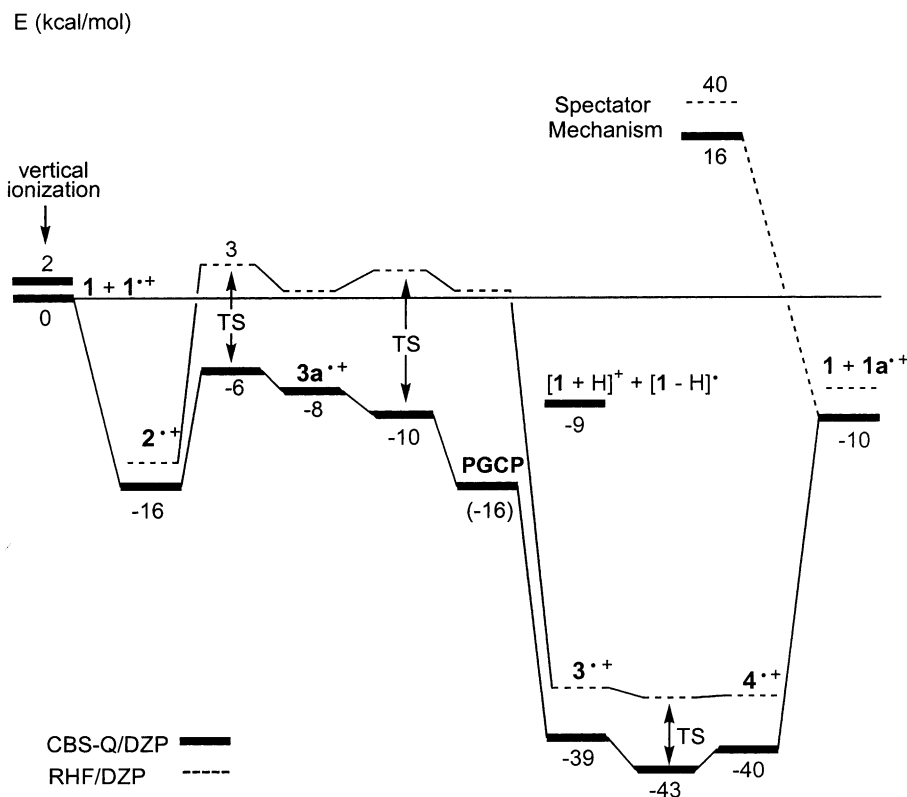
2·+

Me, 1.207, C₁, 146.1, O₂, 2.752, O₃, 1.236, C₄, 106.4, Me
Me
< 1 2 3 4 = −173.2

TS (2 - 3a)·+

Me, 1.230, C₁, 124.7, O₂, 1.190, H₆, 1.444, C₃, 97.9, C₄, 1.388, O₅, 1.284, 120.4, Me, Me
Me
H₈ H₇

< 2 6 3 = 177.8
< 4 3 7 = 114.9
< 4 3 8 = 116.7
< 1 2 3 4 = 169.0
< 2 3 4 5 = − 91.8
< 7 3 4 5 = 19.1
< 8 3 4 5 = 160.3

3a·+

Me, 1.251, C₁, 117.5, O₂, 0.978, H₆, 2.070, H₈, 1.339, C₃, 120.7, C₄, 112.2, Me, O₅, 1.333
Me
H₇

< 2 6 3 = 166.2
< 1 2 3 4 = 76.6
< 2 3 4 5 = − 89.7
< 7 3 4 5 = 7.4
< 8 3 4 5 = 173.0
< 2 6 3 4 = −159.9

TS (3a - 3)·+

< 1 2 3 = 134.3
< 2 3 4 = 97.1
< 1 2 3 4 = 26.1
< 2 3 4 5 = − 55.3
< 6 2 1 3 = 22.1
< 6 2 3 4 = − 26.9
< 7 3 4 5 = 3.2
< 8 3 4 5 = 173.5

Me, 1.256, C₁, 116.9, O₂, 0.962, H₆, 3.253, H₇, H₈, C₃, 1.354, 118.6, C₄, Me, O₅, 1.313
Me

PGCP

< 1 2 3 = 137.6
< 2 3 4 = 91.7
< 4 3 7 = 119.8
< 4 3 8 = 122.0
< 1 2 3 4 = 25.1
< 2 3 4 5 = − 48.0
< 6 2 1 3 = 19.7
< 6 2 3 4 = − 17.4
< 7 3 4 5 = 5.4
< 8 3 4 5 = −177.2

Me, 1.256, C₁, 115.9, O₂, 0.960, H₆, 3.327, H₇, H₈, C₃, 1.345, 116.7, C₄, Me, O₅, 1.325
Me

3·+

Me, 1.244, C₁, 117.8, O₂, 1.007, H₅, 1.503, 137.6, O₃, 1.224, C₄, 120.9, CH₂, 1.458, Me
Me

< 2 5 3 = 176.9
< 1 2 3 4 = 179.9

TS (3 - 4)·+

Me, 1.230, C₁, 122.9, O₂, 1.199, H₅, 1.167, O₃, 124.1, 1.237, C₄, 1.447, CH₂, Me
Me

< 2 5 3 = 179.7
< 1 2 3 4 = 180.4

4·+

Me, C₁, 136.6, O₃, 1.000, H₅, 117.3, 1.254, C₄, 116.4, 1.437, CH₂, Me, Me, 1.216, O₂, 1.528
Me

< 2 5 3 = 176.9
< 1 2 3 4 = 179.9

Spectator TS

Me, C₈, 1.210, O₇, 159.0, 2.407, 2.606, Me, C₁, 1.245, 1.241, O₃, 1.300, 1.304, 1.479, 1.476, C₂, H₅, H₄, 1.366, 1.369, H₆

< 1 2 4	=	76.0	76.2
< 2 4 3	=	100.0	99.5
< 1 3 4	=	87.0	87.4
< 2 1 3	=	96.2	96.8
< 1 2 5	=	116.3	117.6
< 1 2 6	=	117.2	117.6
< 2 1 3 4	=	1.3	0.0
< 5 2 1 3	=	−104.2	−102.8
< 6 2 1 3	=	101.4	102.8
< 3 1 7	=	98.3	
< 2 3 1 7	=	− 86.7	
< 2 1 7 8	=	−148.8	

The *italics* correspond to the monomer TS

Scheme 2.

Fig. 4. Computationally derived energy diagram for the self-catalyzed isomerization of the acetone radical cation $CH_3C(=O)CH_3{}^{\bullet+}$ ($\mathbf{1^{\bullet+}}$) based on calculations at the CBS-Q/DZP (solid lines) and RHF/DZP (dashed lines) levels of theory. Relative energies are given in kcal/mol.

isolated radical also proved unsuccessful. Instead, we find that the PESs for the two forms of the radical have an intersection, where the RHF wave functions of the two radical forms correspond to two different solutions of the RHF equations with the same energy. Calculations on the complex with protonated acetone show the same behaviour, although the energies are affected by the interaction with the charge on the protonated acetone: the alternative form of the radical is stabilized if the hydroxyl group of the protonated acetone points towards the p-electrons of the double bonded CH_2 group in the radical. The transition to the normal form of the radical, as required in order to form ion $\mathbf{3^{\bullet+}}$, is stimulated by moving this hydroxyl group to the oxygen of the radical. The next logical step is then to find the minimum energy crossing

point (MECP) for the intersection, i.e., the geometry corresponding to the minimum energy of the complex with the restriction that the search is confined to the intersection of the two PESs.

However, it turns out that there is a complication in this case, because these calculations lead to geometries which are not useful for defining the transition point for the reaction step at hand. This situation is clarified by Fig. 5. In the usual case, represented by Fig. 5a, optimizations starting from the MECP will lead to different minima, as is the case for a transition state. This follows from the fact that the gradients in the MECP have opposite directions. However, in the situation depicted in Fig. 5b the lower energy points within the intersection have gradients pointing more or less in the *same* direction. As a consequence,

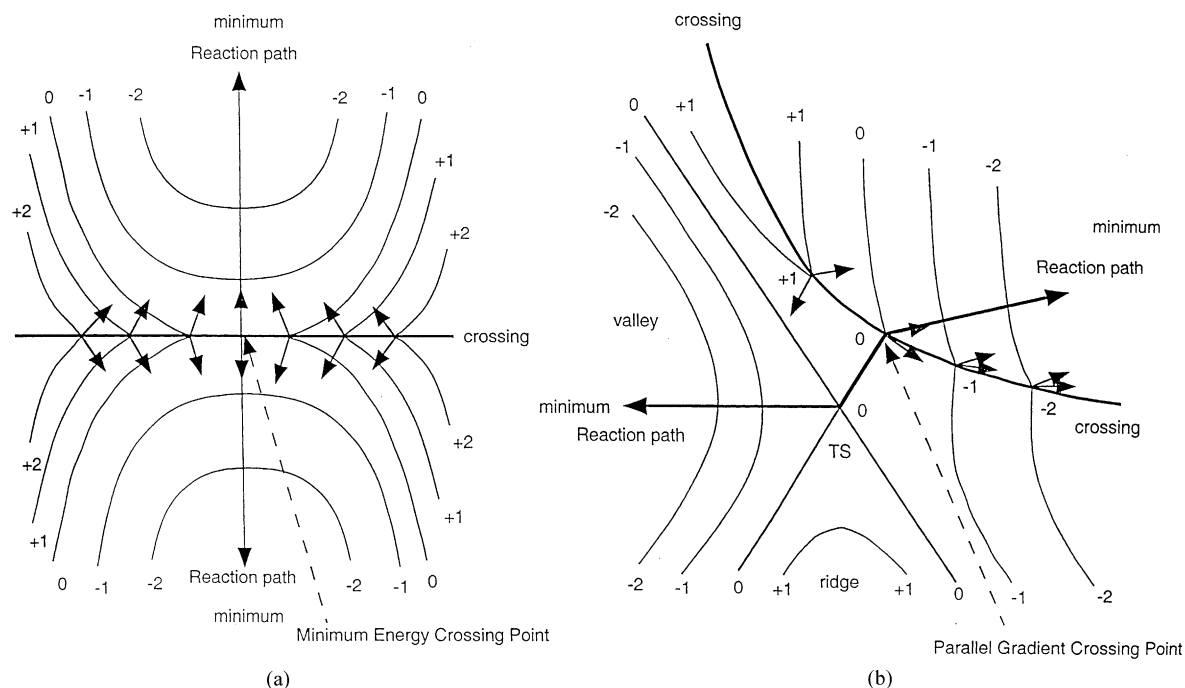MINIMUM → CROSSING → MINIMUM   MINIMUM → TS → CROSSING → MINIMUM

Fig. 5. Schematic potential energy surfaces with an intersection: (a) the minimum energy crossing point is the transition point for the reaction; (b) the parallel gradient crossing point is the transition point for the reaction.

optimizations starting from these points would eventually lead to the *same* minimum. The reason for this behaviour is the fact that the RHF solution corresponding to the upper PES will become unstable if the geometry is too far from the intersection. It will then collapse to the wave function corresponding to the lower PES. As seen in Fig. 5b, a situation with gradients pointing to the same minimum is possible if one of the PESs has a transition state near the intersection. Although the reaction path cannot be defined in a unique way in this situation, useful information may be obtained by monitoring the gradients during the search for the MECP. A reasonable choice for the point where the intersection should be crossed is the point where one of the gradients lies in a plane parallel to the intersection. We will call this point the parallel gradient crossing point (PGCP), see Fig. 5b. In order to find the activation energy for the transition

$3a^{\bullet+} \rightarrow 3^{\bullet+}$, $TS(3a^{\bullet+} \rightarrow 3^{\bullet+})$ in Schemes 1 and 2, it is then necessary to find the transition state indicated in Fig. 5b, starting from the PGCP. This transition state turns out to have virtually the same energy as the PGCP.

As a result, the first step in our mechanism in fact corresponds to a two-step process. In the first step a proton is abstracted from the acetone radical cation without changing the radical site (on the O atom of the radical cation). In the second step the protonated acetone migrates to the O atom of the radical. After passing the $TS(3a^{\bullet+} \rightarrow 3^{\bullet+})$, see Schemes 1 and 2 and Fig. 5b, the complex starts to move in the direction of an O–H–O bridged structure of the form $[CH_3C(O^{\bullet})=CH_2 \cdots HO–C^+(CH_3)_2]$. However, as the protonated acetone approaches the O atom in the radical, the intersection is crossed and the wave function changes character, yielding $3^{\bullet+}$.

Although, this mechanism gives a complete description of the proton transfer catalysis for the enolization of the acetone radical cation, the RHF energies are too high for a satisfactory explanation of the experimental results. Therefore, single point calculations were performed according to the CBS model, using geometries obtained using RHF/DZP instead of UHF/6-31G(d′), as in the CBS-Q model. According to these calculations, the first step TS($2^{\bullet+} \to 3a^{\bullet+}$), abstraction of the proton from the acetone radical cation, is rate-determining with all other transition states and the PGCP being lower in energy. This is in full agreement with experiment from which it was concluded that proton abstraction is rate-determining. We also find that the energy found for TS($3^{\bullet+} \to 4^{\bullet+}$), the $O \cdots H^+ \cdots O$ proton transfer concluding the enolization, is lower than the energies for the ions $3^{\bullet+}$ and $4^{\bullet+}$, indicating that the O·H·O bridge corresponds to a single minimum potential. The energy level of the highest transition state in Fig. 5, TS($2^{\bullet+} \to 3a^{\bullet+}$), lies 6 kcal/mol below that of the reactants $1^{\bullet+} + 1$. Theory, therefore, predicts that the proton transport catalysis may occur at threshold, as is observed.

Also included in Fig. 4 are the results for calculations using a spectator model. The RHF and CBS-Q calculations both predict that the enolization barrier associated with this model greatly exceeds that associated with proton transport catalysis and so the spectator mechanism is not expected to play a role in this system.

4. Conclusions

The acetone radical cation $CH_3C(=O)CH_3^{\bullet+}$ ($1^{\bullet+}$)which, because of a large barrier, does not rearrange to its more stable enol form $CH_2=C(OH)CH_3^{\bullet+}$ ($1a^{\bullet+}$) on its own, can be induced to tautomerize by the interaction of a neutral acetone molecule. Labeling experiments show that the associated mechanism can be viewed as a 1,3-H shift taking place within the acetone dimer radical cation. Ab initio calculations indicate that the process actually occurs via proton transport catalysis. The neutral acetone partner first abstracts a proton from the acetone radical cation and then donates this proton back to the oxygen atom of the incipient $CH_3C(=O)CH_2^{\bullet}$ radical. This process occurs via a "transition state to minimum crossing" as opposed to a conventional "minimum to minimum crossing". Enolization via a spectator mechanism lies too high in energy to compete with proton transport catalysis.

References

[1] P. Longevialle, Principes de la Spectrométrie de Masse des Substances Organiques, Masson, Paris, 1980.
[2] J.L. Holmes, F.P. Lossing, J. Am. Chem. Soc. 104 (1982) 2648.
[3] (a) F. Tureček, C.J. Cramer, J. Am. Chem. Soc. 117 (1995) 12243;
(b) D. Lee, C.K. Kim, B.S. Lee, B.C. Lee, J. Comput. Chem. 18 (1997) 56.
[4] (a) D.H. Williams, Acc. Chem. Res. 10 (1977) 280;
(b) P.C. Burgers, J.L. Holmes, Org. Mass Spectrom. 17 (1982) 123.
[5] (a) D.K. Bohme, Int. J. Mass Spectrom. Ion Proc. 115 (1992) 95;
(b) P. Mourgues, H.E. Audier, D. Leblanc, S. Hammerum, Org. Mass Spectrom. 28 (1993) 1098;
(c) H.E. Audier, D. Leblanc, P. Mourgues, T.B. McMahon, S. Hammerum, J. Chem. Soc. Chem. Commun. (1994) 2329;
(d) H.E. Audier, J. Fossey, P. Mourgues, T.B. McMahon, S. Hammerum, J. Chem. Phys. 100 (1996) 18380;
(e) M.A. Trikoupis, J.K. Terlouw, P.C. Burgers, J. Am. Chem. Soc. 120 (1998) 12131;
(f) M.A. Trikoupis, D.J. Lavorato, J.K. Terlouw, P.J.A. Ruttink, P.C. Burgers, Eur. Mass Spectrom. 5 (1999) 431;
(g) G. Van der Rest, P. Mourgues, J. Tortajada, H.E. Audier, Int. J. Mass Spectrom. 179/180 (1998) 293;
(h) J. Chamot-Rooke, G. Van der Rest, P. Mourgues, H.E. Audier, Int. J. Mass Spectrom. 195/196 (2000) 385;
(i) M.A. Trikoupis, P.C. Burgers, P.J.A. Ruttink, J.K. Terlouw, Int. J. Mass Spectrom. 210/211 (2001) 489;
(j) P. Mourgues, J. Chamot-rooke, G. van der Rest, H. Nedev,

H.-E. Audier, T.B. McMahon, Int. J. Mass Spectrom. 210/211 (2001) 429.

[6] (a) J.W. Gauld, H. Audier, J. Fossey, L. Radom, J. Am. Chem. Soc. 118 (1996) 6299;
(b) J.W. Gauld, L. Radom, J. Am. Chem. Soc. 119 (1997) 9831;
(c) A.J. Chalk, L. Radom, J. Am. Chem. Soc. 121 (1999) 1574.

[7] (a) P.J.A. Ruttink, P.C. Burgers, Org. Mass Spectrom. 28 (1993) 1087;
(b) P.C. Burgers, L.M. Fell, A. Milliet, M. Rempp, P.J.A. Ruttink, J.K. Terlouw, Int. J. Mass Spectrom. Ion Proc. 167/168 (1997) 291;
(c) P.J.A. Ruttink, P.C. Burgers, L.M. Fell, J.K. Terlouw, J. Phys. Chem. A 102 (1998) 2977.

[8] (a) S.G. Lias, J.E. Bartmess, J.F. Liebman, J.L. Holmes, R.O. Levin, W.G. Mallard, J. Phys. Chem. Ref. Data 17 (1988) (Suppl. 1);
(b) S.G. Lias, E.P.L. Hunter, J. Phys. Chem. Ref. Data 27 (1998) (3)

[9] E.L. Clennan, P. Dobrowolski, A. Green, J. Am. Chem. Soc. 117 (1995) 9800.

[10] Gaussian 98, Revision A.7, M.J. Frisch, G.W. Trucks, H.B. Schlegel, G.E. Scuseria, M.A. Robb, J.R. Cheeseman, V.G. Zarzewski, J.A. Montgomery Jr., R.E. Stratmann, J.C. Burant, S. Dapprich, J.M. Millam, A.D. Daniels, K.N. Kudin, M.C. Strain, O. Farkas, J. Tomasi, V. Barone, M. Cossi, R. Cammi, B. Mennucci, C. Pomelli, C. Adamo. S. Clifford, J. Ochterski, G.A. Petersson, P.Y. Ayala, Q. Cui, K. Morokuma, D.K. Malick, A.D. Rabuck, K. Raghavachari, J.B. Foresman, J. Cioslowski, J.V. Ortiz, A.G. Baboul, B.B. Stefanov, G. Liu, A. Liashenko, P. Piskorz, I. Komaromi, R. Gomperts, R.L. Martin, D.J. Fox, T. Keith, M.A. Al-Laham, C.Y. Peng, A. Nanayakkara, C. Gonzalez, M. Challacombe, P.M.W. Gill, B. Johnson, W. Chen, M.W. Wong, J.L. Andres, C. Gonzalez, M. Head-Gordon, E.S. Replogle, J.A. Pople, Gaussian Inc., Pittsburgh, PA, 1998.

[11] (a) M. Dupuis, D. Spangler, J. Wendolowski, NRCC Software Catalogue 1 Program No. QG01, GAMESS, 1980;
(b) M. Guest, J. Kendrick, GAMESS User Manual, An Introductory Guide, CCP/86/1, Daresbury Laboratories, 1986.

[12] (a) J.W. Ochterski, G.A. Petersson, J.A. Montgomery Jr., J. Chem. Phys. 104 (1996) 2598;
(b) J.A. Montgomery Jr., M.J. Frisch, J.W. Ochterski, G.A. Petersson, K. Raghavachari, V.G. Zakrzewski, J. Chem. Phys. 109 (1998) 6505.

[13] N. Heinrich, H. Schwarz, Int. J. Mass Spectrom Ion Proc. 79 (1987) 295.